

# Generation, Characterization, and Reactivity of a Cu<sup>II</sup>–Alkylperoxide/Anilino Radical Complex: Insight into the O–O Bond Cleavage Mechanism

Sayantan Paria,<sup>†</sup> Takehiro Ohta,<sup>‡</sup> Yuma Morimoto,<sup>†</sup> Takashi Ogura,<sup>‡</sup> Hideki Sugimoto,<sup>†</sup> Nobutaka Fujieda,<sup>†</sup> Kei Goto,<sup>¶</sup> Kaori Asano,<sup>§</sup> Takeyuki Suzuki,<sup>§</sup> and Shinobu Itoh<sup>\*,†</sup>

<sup>†</sup>Department of Material and Life Science, Division of Advanced Science and Biotechnology, Graduate School of Engineering, Osaka University, 2-1 Yamada-oka, Suita, Osaka 565-0871, Japan

<sup>‡</sup>Picobiology Institute, Graduate School of Life Science, University of Hyogo, RSC-UH LP Center, Koto 1-1-1, Sayo-cho, Sayo-gun, Hyogo 679-5148, Japan

<sup>¶</sup>Department of Chemistry, Graduate School of Science and Engineering, Tokyo Institute of Technology, 2-12-1 Ookayama, Meguro-ku, Tokyo 152-8551, Japan

<sup>§</sup>Comprehensive Analysis Center, The Institute of Scientific and Industrial Research (ISIR), Osaka University, 8-1 Mihogaoka, Ibaraki, Osaka 567-0057, Japan

## Supporting Information

**ABSTRACT:** The reaction of [Cu<sup>I</sup>(TIPT<sub>3</sub>tren)(CH<sub>3</sub>CN)]ClO<sub>4</sub> (**1**) and cumene hydroperoxide (C<sub>6</sub>H<sub>5</sub>C(CH<sub>3</sub>)<sub>2</sub>OOH, ROOH) at –60 °C in CH<sub>2</sub>Cl<sub>2</sub> gave a Cu<sup>II</sup>–alkylperoxide/anilino radical complex **2**, the formation of which was confirmed by UV–vis, resonance Raman, EPR, and CSI-mass spectroscopy. The mechanism of formation of **2**, as well as its reactivity, has been explored.

Copper–active-oxygen species play versatile roles in a variety of biological and chemical oxidation/oxygenation reactions.<sup>1–3</sup> So far, several types of supporting ligands have been developed to examine copper(I)/dioxygen reactivity as well as copper(II)/peroxide reactivity, providing important information about the structure, physical properties, and reactivity of the reactive intermediates involved in those reactions.<sup>4–6</sup> However, little attention has been focused on noninnocent supporting ligands in the oxygen-activation chemistry by copper complexes.

In this study, we have developed a mononuclear copper(I) complex **1** supported by an N<sub>4</sub>-tetradentate ligand, TIPT<sub>3</sub>tren, consisting of three bulky substituents TIPT (3,5-bis(2,6-diisopropylphenyl)phenyl) and tren (tris(2-aminoethyl)amine) (Figure 1). The reaction of **1** with cumene hydroperoxide (ROOH) at a low temperature gave an unprecedented Cu<sup>II</sup>–alkylperoxide/anilino radical complex **2** (Scheme 1), where the noninnocent aniline moiety of the ligand played crucial roles. The mechanism of formation of **2**, as well as its reactivity, is reported in this *Communication*.

Copper(I) complex **1** was synthesized by mixing an equimolar amount of ligand TIPT<sub>3</sub>tren and [Cu<sup>I</sup>(CH<sub>3</sub>CN)<sub>4</sub>]-ClO<sub>4</sub> in acetone. Single crystals of **1** suitable for X-ray diffraction analysis were obtained as a BF<sub>4</sub><sup>–</sup> salt (for synthetic procedures and characterizations, see Experimental Section and Figures S1–S8 in Supporting Information).

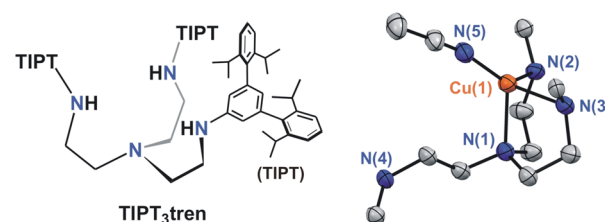


**Figure 1.** ChemDraw structure of TIPT<sub>3</sub>tren ligand (left) and ORTEP drawing of the crystal structure of the core domain of complex **1** (right), where only the carbon atoms connected to the aniline nitrogen atoms, N(2), N(3), and N(4), of the TIPT substituents are shown. All hydrogen atoms and counteranion are also omitted for clarity. For the whole structure, see Supporting Information.

## Scheme 1. Reaction of Complex **1** with Cumene Hydroperoxide

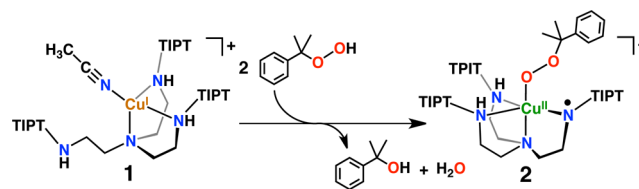


Figure 1 shows the crystal structure of **1**, where copper(I) center exhibits a distorted tetrahedral geometry ligated by three nitrogen atoms, N(1), N(2), and N(3), of the ligand and one nitrogen atom, N(5), of acetonitrile molecule ( $\tau_4 = 0.73$ ,  $\tau_4 = [(360^\circ - (\alpha + \beta))/141^\circ]$ , where  $\alpha$  and  $\beta$  are the two largest bond angles of four-coordinate structure. For an ideal tetrahedral geometry,  $\tau_4 = 1$ , and for a perfect square planar geometry,  $\tau_4 = 0$ ).<sup>7</sup> Thus, one of the ligand arms, N(4), is detached from the copper ion. The FAB-mass spectrum of the

Received: April 21, 2015

Published: August 20, 2015

complex showed a molecular ion peak cluster at  $m/z = 1397.98$ , which matched with a molecular composition of  $[(\text{TIPT}_3\text{tren})\text{-Cu}]^+$  (Figure S7).

The reaction of **1** with cumene hydroperoxide ( $\text{C}_6\text{H}_5\text{C}(\text{CH}_3)_2\text{OOH} = \text{ROOH}$ ) was then examined. Addition of an excess amount of ROOH to **1** at  $-60^\circ\text{C}$  in  $\text{CH}_2\text{Cl}_2$  under anaerobic conditions resulted in formation of a metastable intermediate **2** exhibiting intense absorption bands at 396 nm ( $\epsilon = 5400 \text{ M}^{-1} \text{ cm}^{-1}$ ), 465 nm ( $6000 \text{ M}^{-1} \text{ cm}^{-1}$ ), and 748 nm ( $6600 \text{ M}^{-1} \text{ cm}^{-1}$ ) (Figure 2). The reaction obeyed pseudo-first-order kinetics, and from a linear plot of  $k_{\text{obs}}$  vs  $[\text{ROOH}]$  was obtained a second-order rate constant  $k_2 = 1.67 \pm 0.06 \text{ M}^{-1} \text{ s}^{-1}$  (Figure S9).

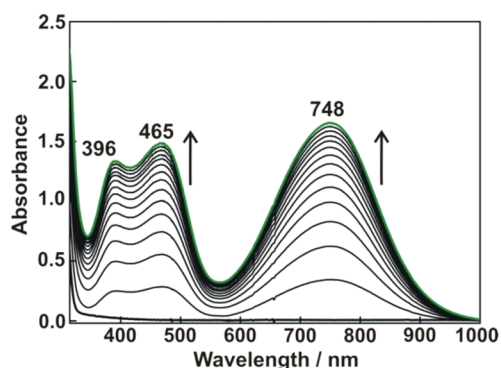


**Figure 2.** UV-vis spectral changes observed upon addition of ROOH (10 equiv) to **1** (0.25 mM) in  $\text{CH}_2\text{Cl}_2$  at  $-60^\circ\text{C}$  under anaerobic conditions.

Product analysis of organic compounds by HPLC (Figure S10) after quenching the reaction at  $-60^\circ\text{C}$  revealed nearly quantitative formation of cumyl alcohol ( $\text{C}_6\text{H}_5\text{C}(\text{CH}_3)_2\text{OH}$ ) (98% based on **1**) together with a trace amount of acetophenone ( $\text{C}_6\text{H}_5\text{C}(\text{O})\text{CH}_3$ ). The quantitative formation of cumyl alcohol (ROH) indicated that the reaction formally involved a heterolytic O–O bond cleavage of the alkylperoxide moiety.<sup>8</sup>

The X-band EPR spectrum of the reaction solution indicated that most of the species in the solution were EPR silent, although a small amount of a  $\text{Cu}^{\text{II}}$  signal ( $\sim 20\%$ ) was observed (Figure S11) probably due to a decomposition product of copper complex intermediate.

The resonance Raman spectrum obtained with 488 nm excitation laser light gave isotope sensitive Raman bands at 831 (Fermi doublet), 604, 569, and 541  $\text{cm}^{-1}$ , which shifted to 788, 589, 558, and 531  $\text{cm}^{-1}$  ( $\Delta\nu = 43, 15, 11, \text{ and } 10 \text{ cm}^{-1}$ ), respectively, upon using isotope labeled cumene hydroperoxide ( $\text{C}_6\text{H}_5\text{C}(\text{CH}_3)_2(^{18}\text{O})_2\text{H}$ ,  $\text{R}(^{18}\text{O})_2\text{H}$ ) (Figure 3a,b). On the basis of the analogy of the resonance Raman features with those of reported  $\text{Cu}^{\text{II}}$ -alkylperoxide complexes,<sup>8–11</sup> a similar type of alkylperoxide complex may be generated in the present reaction. Thus, the band at 831  $\text{cm}^{-1}$  is assigned to the O–O stretching vibrations, whereas the band at 604  $\text{cm}^{-1}$  is due to the Cu–O stretching vibration. Furthermore, the bands around the lower frequency region are attributable to the carbon skeleton deformation (C–C–C/O–C–C), (C–C–C/O–C–C) modes. The isotope shifts of these two bands (569–558 and 541–531  $\text{cm}^{-1}$ ) observed by using  $\text{R}(^{18}\text{O})_2\text{H}$  indicate the presence of significant coupling of the C–C–C/O–C–C deformation modes with the Cu–O stretching mode.<sup>9</sup>

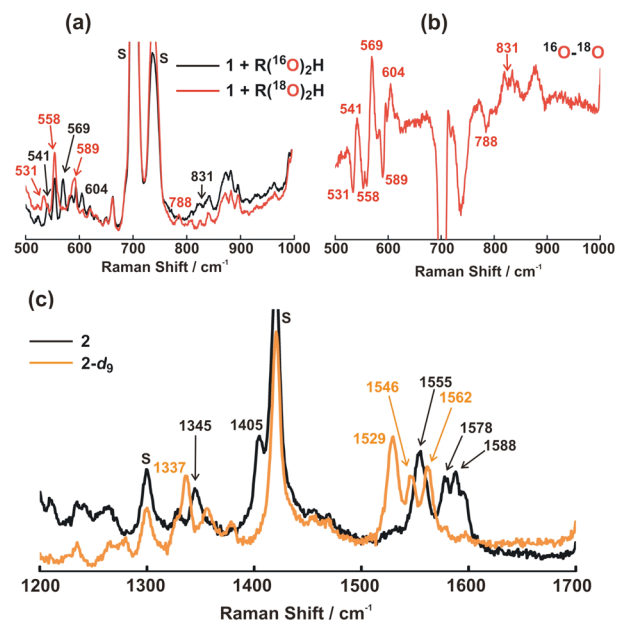


**Figure 3.** Resonance Raman spectra of (a) **2** (black) and its  $^{18}\text{O}$ -derivative (red), (b) a difference spectrum ( $^{16}\text{O} - ^{18}\text{O}$ ), and (c) **2** (black) and its ligand-deuterated derivative **2-d<sub>9</sub>** (orange).

Inspection of the resonance Raman spectrum at the higher frequency region revealed the presence of several bands between 1300 and 1600  $\text{cm}^{-1}$  (1588, 1578, 1555, 1405, and 1345  $\text{cm}^{-1}$ ; Figure 3c, black line spectrum). Importantly, no  $^{18}\text{O}$ -isotope shift was observed in the  $^{18}\text{O}$ -isotope labeled intermediate **2** (Figure S12), clearly indicating that the origin of these bands is not the  $\text{Cu}^{\text{II}}$ -alkylperoxide moiety. Notably, these Raman bands are very similar to those reported for metal-bound anilino radical species, where the bands have been assigned to the C–C and C–N stretching vibrations of the anilino radical moiety.<sup>12,13</sup> To confirm this possibility, we have prepared a deuterated ligand at the 2,4,6-positions of the aniline rings of all the TIPT<sub>3</sub>tren-*d*<sub>9</sub> (Figures S5–S8), and examined the resonance Raman spectrum (Figure 3c, orange line spectrum) of the ROOH adduct intermediate. In this case, we observed prominent peak shifts to 1562, 1546, 1529, and 1337  $\text{cm}^{-1}$ , respectively. The result confirmed that the bands at the higher frequency region were due to the anilino ligand radical bound to the  $\text{Cu}^{\text{II}}$  ion. Considering the resonance structure of the anilino radical moiety, the band at 1588  $\text{cm}^{-1}$ , which shifted to 1562  $\text{cm}^{-1}$  in the deuterated derivative **2-d<sub>9</sub>**, can be assigned to the  $\text{C}_{\text{ortho}}\text{--C}_{\text{meta}}$  ( $\nu_{8a}$ ) stretching vibration. The other band at 1578  $\text{cm}^{-1}$  (shifted to 1546  $\text{cm}^{-1}$ ) was tentatively assigned to the  $\nu_{19a}$  vibration mode. Then, the most intense band at 1555  $\text{cm}^{-1}$  has been assigned to C–N stretching vibration ( $\nu_{7a}$ ), which shifted to 1529  $\text{cm}^{-1}$  in the deuterated derivative. The band at 1405  $\text{cm}^{-1}$  disappeared in the deuterated derivative, suggesting that the band has significant contribution to C–H bending motion, thus assigned to the Wilson  $\nu_{14}$  mode.<sup>14</sup> The vibration at 1345  $\text{cm}^{-1}$  could be assigned to the nontotally symmetric  $\nu_{19b}$  mode, which shifted to 1337  $\text{cm}^{-1}$  in the deuterated intermediate.<sup>14,15</sup> These assignments of the Raman data were well supported by the DFT calculations (Figure S25, Table S3). It was also noted that the O–O/Cu–O stretching modes at 831 and 604  $\text{cm}^{-1}$  slightly shifted to 828 and 606  $\text{cm}^{-1}$ , respectively, in the deuterated intermediate **2-d<sub>9</sub>**, suggesting a direct interaction

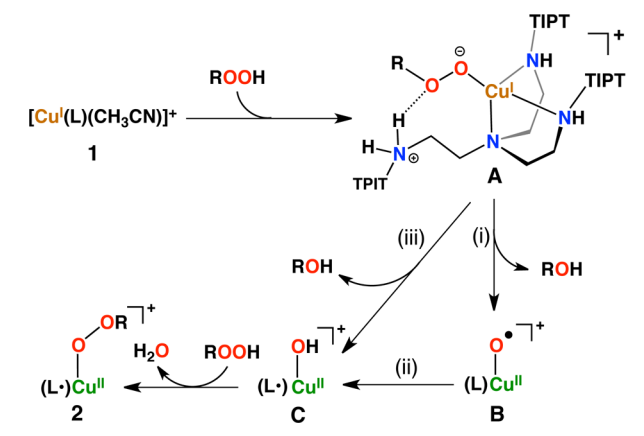
between the anilino radical and  $\text{Cu}^{\text{II}}\text{-OOR}$  moieties (Figure S13a,b).

All these results are consistent with the assignment of compound **2** as a  $\text{Cu}^{\text{II}}$ -alkylperoxide/anilino radical complex as illustrated in Scheme 1. The intense absorption bands in the visible to near-IR region shown in Figure 2 can be assigned to  $\pi \rightarrow \pi^*$  transitions of the metal bound organic radical and an anilino radical to  $\text{Cu}^{\text{II}}$  as well as an alkylperoxide to  $\text{Cu}^{\text{II}}$  charge transfer transitions. The EPR silence of **2** may be due to antiferromagnetic coupling between  $\text{Cu}^{\text{II}}$  and anilino radical as in the case of the oxidized form of galactose oxidase, in which there is a strong antiferromagnetic coupling between  $\text{Cu}^{\text{II}}$  and coordinating phenoxyl radical species, thus being EPR silent.<sup>16,17</sup>

In support of this assignment, the CSI (cold-spray ionization)-mass spectrum of intermediate **2** measured in  $\text{CH}_2\text{Cl}_2$  at  $-60^\circ\text{C}$  showed a peak cluster at  $m/z = 1550$ , the isotope distribution pattern of which is consistent with the molecular component of  $[\text{Cu} + \text{TIPT}_3\text{tren} + \text{C}_6\text{H}_5\text{C}(\text{CH}_3)_2\text{OOH}]$  (Figure S14). Upon use of the isotope labeled cumene hydroperoxide ( $\text{R}^{18}\text{O}_2\text{H}$ ), the peak cluster was shifted by four mass unit (Figure S15), clearly demonstrating that **2** is an alkylperoxide-adduct.

A possible mechanism for the formation of **2** is presented in Scheme 2. Addition of  $\text{ROOH}$  to complex **1** initially forms a

Scheme 2. Proposed Mechanism for the Formation of **2**

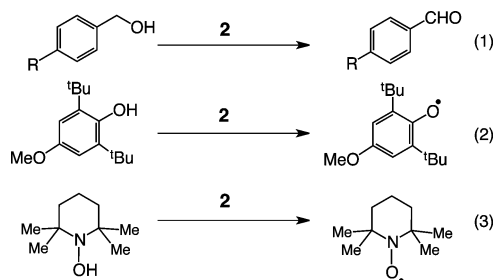


peroxide adduct **A** by replacing the coordinating  $\text{CH}_3\text{CN}$  by  $\text{ROOH}$ . In this step, the noncoordinating ligand arm of **1** ( $\text{N}(4)$  in Figure 1) may act as a base to accept proton from  $\text{ROOH}$  to promote its coordination to  $\text{Cu}^{\text{I}}$ . The resulting ammonium group ( $\text{TIPT-NH}_2^+$ ) may stabilize the alkylperoxide adduct **A** via an intramolecular hydrogen bonding interaction. Then, the heterolytic  $\text{O-O}$  bond cleavage takes place to give  $(\text{L})\text{Cu}^{\text{II}}\text{-O}\cdot$  (intermediate **B**) and  $\text{ROH}$  (path (i)), which may be assisted by the ammonium group ( $\text{TIPT-NH}_2^+$ ) as a general acid catalyst. In fact, the reaction did not occur at all in the presence of base such as triethylamine or 2,6-lutidine. The added base may abstract proton from the ammonium group to prevent the intramolecular hydrogen bonding interaction and the intramolecular general acid catalysis. The generated intermediate **B** immediately abstracts one of the hydrogen atoms of the anilino moieties to give  $(\text{L}^\bullet)\text{Cu}^{\text{II}}\text{-OH}$  (intermediate **C**), where  $\text{L}^\bullet$  denotes the ligand anilino radical (path (ii)). A concerted mechanism is also possible for the generation of **C** from **A** directly (path (iii)). Intermediate **C** undergoes ligand exchange reaction of the

$\text{-OH}$  group with another equivalent of  $\text{ROOH}$  to give the final product **2**. In fact, almost 2 equiv of  $\text{ROOH}$  is needed to get a quantitative formation of complex **2** (Scheme 1). The reaction of an  $\text{M-OH}$  complex with alkyl/acyl peroxide is well-known in the literature.<sup>18,19</sup> Although an iron(IV)-oxo intermediate supported by a ligand radical is known for the porphyrin system,<sup>20</sup> and Peters et al. have recently reported a mononuclear  $\text{Cu}(\text{I})$ -radical complex,<sup>21</sup> compound **2** represents a unique example of a metastable peroxide-complex supported by a nonporphyrin organic radical.

Reactivity of the copper(II)-alkylperoxide/anilino radical complex **2** toward alcohols was examined, since **2** has a similar structural motif with the active form of galactose oxidase as mentioned above. Complex **2** readily reacted with an excess amount (20 equiv) of 4-methylbenzyl alcohol at  $-45^\circ\text{C}$  (Figure S18a) to give 4-methylbenzaldehyde (Scheme 3-1) together with cumyl alcohol as confirmed by HPLC and  $^1\text{H-NMR}$  spectroscopy (Figures S19 and S20).

Scheme 3. Reactivity of Complex **2** toward External Substrates



The decay of absorption bands due to **2** obeyed pseudo-first-order kinetics as shown in Figure S18b, and plot of the pseudo-first-order rate constants  $k_{\text{obs}}$  against the substrate concentration  $[\text{ArCH}_2\text{OH}]$  gave a linear correlation, from which the second-order rate constant  $k_2 = 0.57 \pm 0.03 \text{ M}^{-1} \text{ s}^{-1}$  was obtained from the slope (Figure S18c). The Hammett analysis (plot of  $\log k_2$  vs Hammett constant  $\sigma_p^+$ ) using a series of *p*-substituted benzyl alcohols ( $-\text{OCH}_3$ ,  $-\text{CH}_3$ ,  $-\text{F}$ ,  $-\text{Cl}$ ) gave a Hammett  $\rho$  value of  $-0.42 \pm 0.08$  as indicated in Figure S21. Notably, the Hammett  $\rho$  value of the present reaction is very close to that of the oxidation of benzyl alcohol derivatives by galactose oxidase ( $\rho = -0.09 \pm 0.32$ ),<sup>22</sup> suggesting that the mechanism of the present reaction is similar to that of galactose oxidase.<sup>22</sup> Namely, the alcohol substrate initially replaces the alkylperoxide ligand ( $\text{ROO}^-$ ) to give an alkoxide adduct (Scheme S1). Then, inner sphere electron transfer takes place from the coordinated alkoxide to  $\text{Cu}^{\text{II}}$ , generating an alkoxyl radical intermediate, from which benzylic hydrogen atom is abstracted by the anilino radical moiety to give the aldehyde product. This event produces starting copper(I) complex **1**, from which **2** is regenerated according to the reaction pathways shown in Scheme 2. In fact, the reaction proceeded in a catalytic manner to give 4-methylbenzaldehyde in a 350% yield based on the copper complex after a prolonged reaction time (1 h) at  $25^\circ\text{C}$ .

Complex **2** also reacted with typical hydrogen atom donors such as 2,6-di-*tert*-butyl-4-methoxyphenol (Scheme 3-2) and 2,2,6,6-tetramethylpiperidine-1-ol (TEMPOH, Scheme 3-3) at a low temperature to give 2,6-di-*tert*-butyl-4-methoxyphenoxyl radical and TEMPO $\cdot$ , respectively, as confirmed by UV-vis

and/or EPR spectroscopy, respectively (Figures S22 and S23), further demonstrating the radical character of **2**. Notably, the three absorption bands due to **2** ( $\lambda_{\text{max}} = 396, 465, \text{ and } 748 \text{ nm}$ ) decayed in the same rate in each reaction (eqs 1–3 in Scheme 3, see Figures S18b, S22b, and S23b). The results clearly indicate that the three absorption bands shown in Figure 2 arise from one species, that is complex **2**, but not from a mixture of multiple compounds.

In summary, we have developed a novel Cu<sup>II</sup>–alkylperoxide/anilino radical complex **2**, which represents the first example of a metal–alkylperoxide species supported by a noninnocent ligand radical. For the formation of **2**, the bulky TIPT substituents prohibit undesirable dimerization reaction and one of the alkylamine arms is dissociated from the copper ion to dictate acid–base catalysis for the formation of Cu<sup>I</sup>–OOR and following O–O bond heterolytic cleavage (Scheme 2). Complex **2** induces catalytic oxidation of benzyl alcohol derivatives, presumably through a similar mechanism of galactose oxidase. Further studies are now being undertaken to explore the in-depth reactivity of this novel intermediate.

## ■ ASSOCIATED CONTENT

### 📄 Supporting Information

The Supporting Information is available free of charge on the ACS Publications website at DOI: 10.1021/jacs.5b04104.

Experimental details and additional data (PDF)

## ■ AUTHOR INFORMATION

### Corresponding Author

\*shinobu@mls.eng.osaka-u.ac.jp

### Notes

The authors declare no competing financial interest.

## ■ ACKNOWLEDGMENTS

This work was partly supported by a JSPS fellowship for overseas researchers (to S.P.) and Grants 22105007 (to S.I.) and 24109015 (to H.S.) for Scientific Research on Innovative Areas from MEXT of Japan. The authors also express their gratitude to Prof. Shunichi Fukuzumi and Dr. Kei Ohkubo of Osaka University for their help in EPR measurement.

## ■ REFERENCES

- (1) *Copper-Oxygen Chemistry*; Karlin, K. D., Itoh, S., Eds.; John Wiley & Sons, Inc.: Hoboken, NJ, 2011; Vol. 4.
- (2) Solomon, E. I.; Heppner, D. E.; Johnston, E. M.; Ginsbach, J. W.; Cirera, J.; Qayyum, M.; Kieber-Emmons, M. T.; Kjaergaard, C. H.; Hadt, R. G.; Tian, L. *Chem. Rev.* **2014**, *114*, 3659–3853.
- (3) Lee, J. Y.; Karlin, K. D. *Curr. Opin. Chem. Biol.* **2015**, *25*, 184–193.
- (4) Lewis, E. A.; Tolman, W. B. *Chem. Rev.* **2004**, *104*, 1047–1076.
- (5) Mirica, L. M.; Ottenwaelde, X.; Stack, T. D. P. *Chem. Rev.* **2004**, *104*, 1013–1045.
- (6) Itoh, S. *Curr. Opin. Chem. Biol.* **2006**, *10*, 115–122.
- (7) Yang, L.; Powell, D. R.; Houser, R. P. *Dalton Trans.* **2007**, 955–964.
- (8) Tano, T.; Ertem, M. Z.; Yamaguchi, S.; Kunishita, A.; Sugimoto, H.; Fujieda, N.; Ogura, T.; Cramer, C. J.; Itoh, S. *Dalton Trans.* **2011**, *40*, 10326–10336.
- (9) Chen, P.; Fujisawa, K.; Solomon, E. I. *J. Am. Chem. Soc.* **2000**, *122*, 10177–10193.
- (10) Kunishita, A.; Teraoka, J.; Scanlon, J. D.; Matsumoto, T.; Suzuki, M.; Cramer, C. J.; Itoh, S. *J. Am. Chem. Soc.* **2007**, *129*, 7248–7249.
- (11) Choi, Y. J.; Cho, K.-B.; Kubo, M.; Ogura, T.; Karlin, K. D.; Cho, J.; Nam, W. *Dalton Trans.* **2011**, *40*, 2234–2241.

(12) Penkert, F. N.; Weyhermüller, T.; Bill, E.; Hildebrandt, P.; Lecomte, S.; Wieghardt, K. *J. Am. Chem. Soc.* **2000**, *122*, 9663–9673.

(13) Miyazato, Y.; Wada, T.; Muckerman, J. T.; Fujita, E.; Tanaka, K. *Angew. Chem., Int. Ed.* **2007**, *46*, 5728–5730.

(14) Tripathi, G. N. R.; Schuler, R. H. *Chem. Phys. Lett.* **1984**, *110*, 542–545.

(15) Tripathi, G. N. R.; Schuler, R. H. *J. Chem. Phys.* **1987**, *86*, 3795–3800.

(16) Whittaker, J. W. *Chem. Rev.* **2003**, *103*, 2347–2363.

(17) In a parallel-EPR spectrum taken at 4 K, there was no signal around  $g \sim 4$ . All the <sup>1</sup>H and <sup>2</sup>H signals appeared in the diamagnetic region for **2** and 2-*d*<sub>9</sub> in the <sup>1</sup>H and <sup>2</sup>H NMR spectra (Figures S16 and S17). All these results were consistent with the assignment of **2** as a singlet species ( $S = 0$ ). However, a preliminary DFT calculation of complex **2** suggested that the triplet state is more stable than the singlet state by 3.3 kcal mol<sup>-1</sup> (see SI). Thus, further detailed studies are needed to clarify the precise electronic structure of **2**.

(18) Kitajima, N.; Katayama, T.; Fujisawa, K.; Iwata, Y.; Morooka, Y. *J. Am. Chem. Soc.* **1993**, *115*, 7872–7873.

(19) Groves, J. T.; Watanabe, Y. *J. Am. Chem. Soc.* **1988**, *110*, 8443–8452.

(20) *The Porphyrin Handbook: Biochemistry and Binding: Activation of Small Molecules*; Kadish, K. M., Smith, K. M., Guilard, R., Eds.; Academic Press: San Diego, CA, 2000; Vol. 4.

(21) Mankad, N. P.; Antholine, W. E.; Szilagy, R. K.; Peters, J. C. *J. Am. Chem. Soc.* **2009**, *131*, 3878–3880.

(22) Whittaker, M. M.; Whittaker, J. W. *Biochemistry* **2001**, *40*, 7140–7148.